Potential alternative land covers on Earth

Jean-Francois Bastin

bastin.jf@gmail.com

Université de Liège https://orcid.org/0000-0003-2602-7247

Nicolas Latte

https://orcid.org/0000-0002-3822-315X

Claude Garcia

BFH / ETHZ https://orcid.org/0000-0002-7351-0226

Fabio Berzaghi

World Maritime University

Fernando Maestre

University of Alicante https://orcid.org/0000-0002-7434-4856

Jens-Christian Svenning

Aarhus University https://orcid.org/0000-0002-3415-0862

Jan Bogaert

https://orcid.org/0000-0003-4465-6442

Emeline Assede

Université de Parakou

Sabas Barima

Universié Jean Lorougnon Guédé https://orcid.org/0000-0001-9840-6989

Timothée Besisa

ERAIFT

Samuel Bouchoms

Université de Liège

Thalès de Haulleville

Ghent University

Hugo de Lame

Université de Liège https://orcid.org/0000-0002-6598-5854

Pauline Depoortere

Université de Liège

Marc Dufrêne

Université de Liège https://orcid.org/0000-0002-5664-9955

Anne Hoek van Dijke

Max Planck Institute for Biogeochemistry https://orcid.org/0000-0003-0354-8517

Philippe Lejeune
Université de Liège
Simon Lhoest
Université de Liège https://orcid.org/0000-0001-7237-3867
Gregory Mahy
Université de Liège
Christian Messier
Université du Québec à Montréal https://orcid.org/0000-0002-8728-5533
Danilo Mollicone
United Nations Food and Agriculture Organization
Marc Peaucelle
INRAE, Université de Bordeaux https://orcid.org/0000-0003-0324-4628
Antoine Plumacker
Université de Liège https://orcid.org/0009-0006-9767-992X
Fabien Quétier
Rewilding Europe https://orcid.org/0000-0002-3767-0353
Olivia Rakotondrasoa
Université d'Antannarivo https://orcid.org/0000-0001-7263-2363
Felana Ramalason
Université de Liège https://orcid.org/0000-0003-1487-4027
Raoul Sambieni
Université de Liège https://orcid.org/0000-0001-5062-0791
Ben Sparrow
https://orcid.org/0000-0003-2566-1895
Harold Strammer
Université de Liège
Yegor Tarelkin
Université de Liège
Yannick Useni Sikuzani
Université de Lubumbashi https://orcid.org/0000-0003-0508-1180
Arthur Vander Linden
Université de Liège https://orcid.org/0000-0001-5760-9608

Article

Keywords:

Posted Date: February 2nd, 2024

DOI: https://doi.org/10.21203/rs.3.rs-3830372/v1

Additional Declarations: There is **NO** Competing Interest.

Abstract

Preserving and restoring terrestrial ecosystems is crucial to halting the collapse of life on Earth. To guide global conservation and restoration efforts, we present a comprehensive map, encompassing all ecosystems, revealing the Earth's potential tree, short vegetation, and bareground cover accounting for various land management scenarios such as prescribed fire frequency and trophic rewilding. Our analysis indicates that 43% (5678 Mha) of lands could be covered by trees, 39% (5179 Mha) by shrubs and grasses, and 18% (2347 Mha) by bareground. Approximately 1070 Mha can support alternative land covers, emphasizing the need to consider diverse outcomes in landscape restoration. Our findings also suggest that management scenarios may significantly outweigh the average impact of climate change on resulting land covers, underscoring decision-makers' responsibility for nature's recovery and a sustainable future.

Main text

During the last decades, several planetary boundaries have been crossed - in particular those related to biological integrity and climate change[1] - stressing the need for increased biodiversity protection, restoration and adaptation[2–6]. International organizations have now seized its importance, as reflected by the adoption by the General Assembly of the United Nations, on the 1st of March 2019, of a resolution to establish the 2021–2030 period as the "Decade of Ecosystem Restoration". This resolution is also backed by the latest reports of the 6th Assessment Report of the Intergovernmental Panel on Climate Change[2] and by the adoption of global quantitative restoration targets under the Global Biodiversity Framework adopted by the parties of the Convention on Biological Diversity in Montréal in December 2022. While ecosystem restoration is largely supported by governments, NGOs and stakeholders worldwide, restoration actions on the ground largely focus on planting trees through reforestation or afforestation[7]. This bias toward tree planting can lead to unintended negative outcomes for the mitigation of climate change itself, the conservation of other life forms (including vegetation, animals, fungi, and microbes), and the rights and livelihoods of local communities[8]. Examples of negative unwanted impacts include, but are not limited to, warming in boreal regions due to tree cover-induced changes in albedo[9], increased evapotranspiration leading to a loss of water availability[10], lower carbon storage in soils when replacing old-growth grasslands with tree plantations[11], or a collapse in native biodiversity with the replacement of native savannahs by exotic plantations[7]. Hence, developing holistic methods and approaches for ecosystem restoration considering the wider impacts of this activity on nature and local communities and the potential of the land to hold multiple vegetation types is essential to maximize its environmental and socio-economic benefits and to avoid critical mistakes.

Restoration activities can lead to alternative ecosystems in a landscape, which can be obtained by following different management scenarios (e.g., protection, reforestation, reintroduction of keystone species, and the use of prescribed fire or fire exclusion)[12,13]. Restoration should consequently begin with a multiple-choice question: what are the possible alternative ecosystems that can be found within a given

landscape? Answering this question is crucial to maintain complex landscapes and preserve biodiversity[14]. Decision makers who limit the exploration of future possibilities to a single type of ecosystem, whether considering forests or grasslands, risk overlooking other states that may be better adapted for the local biophysical conditions, both now and in the future, as well as for the changing needs and interests of people[15]. For instance, while reforestation may be a viable option in numerous dryland regions today, certain areas that used to harbor trees in the past may not sustain forest ecosystems under future climate conditions[4,16,17]. To maximize the social, environmental and economic benefits of restoration, it is crucial to move beyond a narrow focus on "forest vs. non-forest" possibilities and to explore all potential land cover alternatives accounting for factors such as future climate uncertainty, human livelihoods and the risks and benefits that may arise from restoration outcomes[18]. While recognizing the importance of considering alternative ecosystems for restoration is not new[13,19,20], the lack of a comprehensive global assessment of alternative land covers continues to impede progress in the field and – more critically – reinforce conflicting views on the matter[7,8]. A global assessment of the potential for alternative ecosystems is thus crucial for the development of effective restoration initiatives that maximize the benefits of these actions and minimize undesirable outcomes.

Here, we first created a map showing the potential land area covered by trees, short vegetation (comprising shrubs and grasses), and bareground (areas devoid of perennial vegetation but which might harbor biocrusts and annual plants) globally at a resolution of 0.25 degrees per pixel (Fig. 1). This map, referred as the median potential fractional vegetation cover, is generated using land covers data collected over 40,000 0.5-hectare plots within all protected areas. We choose protected areas to assess the reference state of the different potential land covers considered in any location of the planet, and subsequently guide restoration actions. Many protected areas, however, experience some level of human degradation that might ultimately lead our model to the misrepresentation of the reference state. Degradation can relate to historical and current anthropogenic activities like legal and illegal logging, past defaunation and local extinctions, ongoing poaching or excessive hunting, or increased abundance of exotic pests and diseases[21–23]. To limit the potential resulting bias, we further extrapolate our map considering as a reference state solely those protected areas under conservative IUCN categories I, II and III (i.e. over 18,000 plots; Fig S1).

To predict the fractional vegetation cover, we combined climate variables, soil properties, fire frequency and wildlife herbivory within a neural network modeling framework (see Methods). We employed various climate databases to account for the model's sensitivity to the choice of climatic data and accounted for potential model overfitting (see Methods). To encourage further interpretation and comparison of our results, all datasets were scaled to a pixel resolution of 0.25 degrees. All the models yielded good results, showing a very limited impact (< 1%) of the modelling framework and of the choice of climate dataset and a rather limited (~ 5%) impact of the spatial structure of the training dataset (Figs. S2 and S3). We then generated the final map by extrapolating the model beyond protected areas for each climate data source and calculating the median fractional vegetation cover for each pixel (Fig. S4). Based on the

climate envelope of our model, we estimate here that 95% of the pixels of the median fractional vegetation cover map fall within the range of observed values in the training points (see Methods).

Our study reveals that the median potential fractional vegetation cover of the planet (Fig. 1) is comprised of 5678 (± 79) Mha of trees (43%), 5179 (± 92) Mha of short vegetation (39%), and 2347 (± 66) Mha of bareground (18%). Interestingly, our maps reveal two distinct patterns at the global level (Fig. 1). From tropical to desert regions, each biome tends to be dominated by one potential land cover. Tropical biomes are dominated by trees, subtropical biomes by short vegetation and desert biomes by bareground (Table S1). From temperate to boreal regions, each biome tends to present a more balanced distribution of the land cover, in particular for short vegetation and tree cover. This finding is in line with a recent assessment of the land covers in Europe during the last interglacial period[24], i.e. the youngest period with a similar climate as today and absence of *Homo sapiens*. Tropical and subtropical moist forests have the largest area potentially covered by trees (on average 1,615 Mha), but also present 311 Mha of land potentially covered by short vegetation. Similarly, tropical and subtropical grasslands have the largest area potentially covered by short vegetation (1,125 Mha), but also present 723 Mha of land potentially covered by trees. Desert biomes have significant potential for short vegetation and tree cover, with 1,057 Mha and 408 Mha respectively, with 1307 Mha strictly covered by bareground. This potential for vegetation is nonetheless expected to shrink in desert biomes in the next decades due to forecasted climate and land use changes[4,16]. These results highlight that landscape restoration cannot afford to overlook any type of land cover. Whether in arid, boreal, temperate, or tropical biomes, a restoration project should always consider the opportunity, costs and benefits of restoring different ecosystems, and the possibility of letting restored natural processes determine the outcome. This underscores the remarkable heterogeneity of vegetation on Earth and the intricate challenges associated with their conservation and restoration.

Using multiple realistic fire regimes and wildlife herbivory scenarios, i.e. respecting the observed range of fire intensity and herbivore biomass in each ecoregion of the world (see Methods), we map the potential alternative land covers on Earth (Fig. 2). Each pixel of the map represents the standard deviation of the predictions obtained from the different scenarios for trees, short vegetation, and bareground cover in green, blue, and red, respectively (Fig. 2). The resulting additive color rendering corresponds to landscapes where alternatives are found between two dominant land cover types. In total, the map illustrates that roughly 1070 Mha of the Earth's surface can support alternative land covers, an area equivalent to the total current expanse of tropical moist forest[25]. The most substantial hotspots for alternative potential ecosystems are found in subtropical and temperate biomes, where fire and herbivory scenarios promote the transition from dense forests to grassy systems and eventually from grassy systems to deserts (Fig. 2). These hotspots result mostly from an asymptotic relationship between land cover and fire regime, as an increase of fire will substantially favor short vegetation over trees beyond a certain threshold of fire frequency (Fig S5). The effect of wildlife herbivory appears more complex, as an increase of herbivory biomass is not systematically related to a decrease of tree cover (Fig. S5). Indeed, high herbivore densities can be found both within dense forests (e.g., forest elephants, great apes, etc.)

and herbaceous savannas[26]. High herbivore densities can also increase vegetation heterogeneity and consequently their overall resilience vs. external forcing[27].

Our results provide valuable insights to help guide ecosystem restoration efforts while taking into account the alternative options that together shape complex and heterogeneous landscapes[28]. They can assist stakeholders in assessing how climate change, prescribed fire intensity, fire exclusion, and wildlife herbivory may affect the tree, short vegetation, and bareground cover of a given landscape. This could help guiding existing restoration initiatives such as natural grazing projects in Europe's rewilding landscapes, where we can evaluate the scenario needed to promote more heterogeneous landscapes[29] and address the effects of land abandonment[30], trophic rewilding experiments in Siberia (e.g. 'the Pleistocene park') where grassy ecosystems might stabilize soil temperatures and limit permafrost melting[31], trophic rewilding experiments in African savannah where elephants help promote semi-open ecosystems[32], or reforestation initiatives in Africa aiming to slow down land degradation and desertification (e.g., the Great Green Wall[33]). Using our model considering various fire and herbivory scenarios, together with the average expected climate change by 2050[34], we found that an increase of herbivore biomass up to 30,000 $kg.km^{-2}$ - i.e. close to the upper limit observed in Europe latest interglacial age[35] or about 30 buffalos or six elephants per km^2 - can decrease the tree cover from 55–11% in the Dinaric mountains of Europe, and from 44–8% in the Northeast Siberian Taiga (Fig. 3). Fire prescription or exclusion in West Sudanian savannah might change the potential tree cover by 23%, shifting between 33% and 56% when passing from 0.5 to 0 fire yr^{-1} (Fig. 3). Interestingly, results show that the choice of management action appears to have a much stronger impact on the final land cover than average climate change alone. In this regard, the effects of the average expected climate change by 2050 only changed the resulting land cover of the previous examples by less than 3%. While the maps and model presented here are robust and informative, and given the spatial extent of globally available data, further refinement and validation of our models would enhance their accuracy and usefulness for particular restoration or rewilding initiatives on the ground. Similarly, the inclusion of punctual but extreme climatic events might improve our understanding of the effect of climate change vs. the effect of management action on the resulting land cover.

In conclusion, our findings emphasize that effective and goal-setting restoration strategies hinge upon the comprehensive assessment of the various potential land covers that could coexist in a given landscape. More importantly, they also highlight that land management actions are very likely to outweigh the average effect of climate change on the resulting restoration outcome. As such, we believe that our results can help guiding the design of ecologically and socially responsible landscape restoration initiatives that are required to combat our ongoing climate and biodiversity crises.

Methods

The code used in the present study, including data preparation, model training, validation and evaluation, and mapping is available as an R project on GitHub (Data File S1).

1. Set-up of the study

We set-up a data-driven neural network model to map the Earth´s potential fractional vegetation cover. The model is trained on environmental data in combination with a dataset of land-cover in protected areas of the globe. We used this model to predict land cover based on a range of climatic data sets, herbivory, and fire scenarios.

2. Assessment of land cover

The training dataset corresponds to the augmented photo-interpretation of three types of land cover: trees, short vegetation (including grasses and shrubs), and bare ground. We used data from over 40,000 0.5-hectare plots distributed across the protected areas of the globe (Fig S1) and following a systematic sampling grid design (20 by 20 km). In the model, we further make the distinction between 18,000 plots falling under conservative IUCN categories I, II and III (category = 1) and the rest of the plots falling under IUCN categories IV, V and VI (category = 0). The database, which is accessible as a supplementary material (Data File S1), results from previous studies on the global assessment of dryland forests and the global tree restoration potential [4,36]. Similar to these previous studies, we added plots from the global dryland assessment falling in desert regions to cover the full range of environmental conditions.

3. Augmented visual interpretation of the three land cover categories using Collect Earth

The assessment of land cover in each plot was conducted using the Augmented Visual Interpretation approach with the assistance of Collect Earth [37]. Collect Earth, an open-access software developed by the Open Foris initiative of the Food and Agriculture Organization of the United Nations (FAO), utilizes Google Earth and Google Earth Engine to provide multi-source and multi-level information to facilitate the photo-interpretation of land cover. This software enables the operator to perform photo-interpretation of a 70 x 70 m square plot, combining land cover information derived from satellite images with very high spatial (pixel size ≤ 1 meter) and temporal (daily data acquisition) resolution. To interpret the land cover, the operator utilizes freely accessible, very high spatial resolution, satellite images which can be visualized on Google Earth. Simultaneously, the operator cross-references the interpretations with spectral information obtained from medium-to-high resolution satellite images, including MODIS, Landsat 7/8 from USGS mission, and Sentinel 2 from Copernicus mission, which have been automatically compiled over the past 20 years. In our case, each plot consists of a systematic grid of 7-by-7 points (49 points), allowing convenient and direct estimations of tree cover, short vegetation cover, and bare ground cover. Each point on the grid represents 2% of the plot area. The three land cover values range from 0 to 100% and sum up to 100% for each plot. Distinguishing trees from short vegetation was based on visual assessment of crown size, where crowns width below 2 meters considered as non-tree woody cover. More details on the photo-interpreted inventories we use are provided in previous studies [4,36].

4. Environmental determinants of land cover

To build the global potential distribution of the three land covers and the subsequent global potential alternative land cover map, we further develop an empirical model based on neural network approaches [38] to predict the relationship between environmental determinants (climate, soil, fire regime, and wildlife herbivory) and land cover within protected areas. We detail hereafter the preprocessing of each of the datasets used.

- Protected areas

Similarly to previous studies, we identified regions of the world with limited human activity using the World Database on Protected Areas [39] (WDPA), developed by the United Nations Environmental Program (UNEP) and the International Union for Conservation of Nature (IUCN). These regions are nonetheless not entirely exempt from human activity [40]. Therefore, we distinguish conservative protected areas, from IUCN category I, II and III (category = 1) and the rest (category = 0). Our extrapolated maps, i.e. outside protected areas, are produced considering only the restrictive IUCN categories I, II and III to estimate the potential land cover of the planet with limited human activity.

- Climate data

In the present study, we consider that global climate databases, whether derived from meteorological station records or satellite mission predictions, are prone to uncertainties and biases. To address this potential issue, we have incorporated six global climate reference datasets, namely CHELSA, CRU TS4, ERA5, MODIS, NEX historical and Worldclim [41–45].

For each dataset, we examined four climate variables aggregated over a significant time span of 10 to 30 years (between 1980 and 2010), depending on the availability of the data in each specific database. We considered the total yearly precipitation, the average yearly temperature, and the yearly standard deviation of monthly temperature and precipitation. These variables have been carefully chosen to capture both the annual average conditions and the seasonal patterns in temperature and precipitation. The code for the preparation of these climate dataset and their accessibility are available as a supplementary data file (Data File S1).

- Soil and Topography

To characterize soil properties, we used the ClustOfVar R package [46], to select three soil and two topographic variables out of a total of 34 quantitative soil descriptors derived from soilgrids [47] and five topographic properties derived from GMTED2010 [48]. The final selection of soil and topographic variables include the soil organic carbon stock from 0-to-15 cm, depth to bedrock, sand content from 0-to-15 cm, elevation, and hillshade.

- Fire frequency

We computed fire frequency through Google Earth Engine using the Terra and Aqua combined MCD64A1 Version 6 Burned Area MODIS data product [49]. It is a monthly, global gridded 500 m product containing per-pixel burned-area and quality information. The MCD64A1 burned-area mapping approach employs 500 m MODIS Surface Reflectance imagery coupled with 1 km MODIS active fire observations. Here, we converted the map into a binary yearly information, counting whether a fire was detected or not each year of the period 2001–2020 (Data File S1). We then computed a single map to assess the yearly fire frequency over the 2000–2020 period. The map shows that the African continent is the most subject to fire, particularly in the inter-tropical regions.

- Herbivory dataset

The herbivory dataset is compiled from the study of Berzaghi et al. of 2021 [26], where the authors studied the global distribution of mammal herbivore biomass using dynamic vegetation models calibrated on observed datasets gathered over protected areas. To account for the general trends of herbivore biomass and daily intake in natural systems, we merged the data, that was originally structured in 24 functional groups, into three levels of information, i.e. the estimated dry biomass in kilogram of wet weight per km^2 (i.e., the biomass), the estimated total biomass intake in kg of dry mass$\cdot$ km^{-2} (i.e., the intake) and, finally, the estimated daily litter intake in kg of dry mass per square kilometer. Accounting for the litter intake allows to focus on the impact of herbivores being very dependent of seasonal source of intake (i.e. the littler). The herbivore datasets are available in the Data File S1.

- List of selected variables

Based on aforementioned steps, we select a total of 13 variables, listed as follows: annual average precipitation, average annual temperature, standard deviation of precipitation, standard deviation of temperature, bedrock depth, elevation, hillshade, soil organic carbon content, sand content, fire frequency, herbivore total biomass, herbivore total intake, and herbivore litter intake.

5. The representativity of the training dataset

To assess the representativity of the training dataset, we first assessed the range of the four climatic variables (mean temperature, annual precipitation, precipitation seasonality, and temperature seasonality) used within and outside protected areas per biomes. These ranges illustrate that the protected areas cover well the global variation of these four climatic values (Figs S6-S7). Additionally, we performed a convex hull analysis to account for the co-variations between the four climatic variables. The results obtained show that less than 5% of the terrestrial land on the planet fall beyond the limits of the convex hull, meaning that our counterfactual map is the result of 95% of interpolation and 5% of extrapolation (Data File S1).

6. The neural network model

- Neural network architecture

Our base model is a multilayer perceptron (MLP) based on simple neural networks. The model is composed of two hidden layers (64 features each). Between hidden layers, a “tanh” activation function and a dropout of 0.75 were applied. At the end of the MLP, a "softmax” activation function was applied to reconstruct proportions of the three land covers: trees, short vegetation and bare ground. Input and output data are tabular with one line per photo-interpreted plot for training and one line per pixel of 0.25 degrees for prediction.

- Model training, prediction, and assessment of variabilities

The methodology is defined to avoid model overfitting, to ensure prediction robustness, and to evaluate four potential sources of variability in the mapping of the three land covers: the choice of the climate data source, the effect of the spatial structure of the training dataset, the model uncertainty, and the sensitivity to the scenario of fire and herbivory.

The weighted mean square error (MSE) was used as loss function for training. The weights of the neural networks were computed for balancing the number of samples between continents, IUCN categories (0/1) and vegetation cover classes (highest proportions). The training parameters (number of epochs, learning rate, etc.) were set trough trials and error considering the k-folds cross-validation.

In total, 66 MLPs were trained: 10 (spatial folds) + 1 (all folds) for each of the six climate data sources (CHELSA, CRU TS4, ERA5, MODIS, NEX historical, and Worldclim). The use of the different climate datasets allowed us assessing the sensitivity to the choice of the climate source (Fig. S8 bottom). Similarly, the use of the 10 folds, corresponding to spatially and environmentally separated areas (Fig. S9), generated using the blockCV package in R [50], allowed assessing the sensitivity of our model to the spatial structure of the training dataset (Fig. S8 middle). After training, for each of the 66 MLPs, 10 (dropout activated) + 1 (dropout deactivated) repetitions of predictions were done. These 10 repetitions were used to assess the model variability (uncertainty) (Fig. S8 top). Finally, the predictions were also done considering the fire and herbivory scenarios (5 x 5) to assess the scenario variability (Fig. 2).

To sum up, the six predictions with all folds, dropout disactivated, and median fire and median herbivory scenarios were used to generate the global maps (Fig. 1 and Fig. S4). Other predictions were used to assess the four types of variabilities (Fig. 2 and Fig. S11). For a more detailed description of these variabilities see points 7 to 10 of this supplementary material.

Finally, to consider climate change (CC), supplementary predictions were done using ‘NEX historical’ model [51]. The extrapolations for 2050 were done considering the average of all models considered in the NEX CMIP6 product (i.e. ACCESS-CM2', 'ACCESS-ESM1-5', 'BCC-CSM2-MR', 'CESM2', 'CESM2-WACCM', 'CMCC-CM2-SR5', 'CMCC-ESM2', 'CNRM-CM6-1', 'CNRM-ESM2-1', 'CanESM5', 'EC-Earth3', 'EC-Earth3-Veg-LR', 'FGOALS-g3', 'GFDL-CM4', 'GFDL-ESM4', 'GISS-E2-1-G', 'HadGEM3-GC31-LL', 'HadGEM3-GC31-MM', 'IITM-ESM', 'INM-CM4-8', 'INM-CM5-0', 'IPSL-CM6A-LR', 'KACE-1-0-G', 'KIOST-ESM', 'MIROC-ES2L', 'MIROC6', 'MPI-ESM1-2-HR', 'MPI-ESM1-2-LR', 'MRI-ESM2-0', 'NESM3', 'NorESM2-LM', 'NorESM2-MM', 'TaiESM1', 'UKESM1-0-LL') under the scenario ssp5 (Fig. 3).

- Model evaluation

Model validation was done progressively by analyzing the residuals, the variable importance, and their profiles. A first assessment of the model is presented through the averages and ranges of the model part profiles (Fig S5). This figure shows how, at the global level, each land cover type responds to the variation of standardized model parameters. Interestingly, and despite being an empirical machine-learning model, the figure presents biologically meaningful relationships between the predictive and the response variables, providing confidence in the quality of the model. The comparison of predicted and observed values (Fig. S2) revealed that the models generally present a good and unbiased prediction of each land cover type, yet with a small systematic underestimation of the prediction of high bare ground values.

- Scenarios of fire regime and wildlife herbivory

To model the potential land cover beyond the geographic limits of the world's protected areas, it is necessary to consider potential scenarios of fire regime and herbivory that are currently not present outside protected areas, i.e. counterfactuals. To consider realistic situations, we propose scenarios based on the observed frequency distributions of fire frequency and herbivory within protected areas, calculated for each ecoregion and each biome. For each distribution, we identified very low (5th percentile), low (25th percentile), median (50th percentile), high (75th percentile) and very high values (95th percentile 95th).

- Biomes and terrestrial ecoregions

The scenarios of fire regime and wildlife herbivory are built from observations within protected areas and are considered per biome and terrestrial ecoregion -as defined by Olson and colleagues [52]-, as these consist of large units of land containing distinct natural communities and species. We therefore assume that the fire regime and the wildlife herbivory observed within the protected areas of these biomes/ecoregions are realistic scenarios of fire and herbivory that could be implemented for a restoration project at the scale of the biomes/ecoregions.

7. The median potential fractional vegetation cover map

The median potential fractional vegetation cover represents the median case scenario of the distribution of bare ground (red), tree (green) and short vegetation (blue) cover (Fig. 1), produced considering the different climate source data and considering a median scenario of fire and herbivory. One map was produced for each climate reference database, and the resulting final map corresponds to the median pixel value calculated from these maps (Fig S4).

8. Variability maps and variability assessment

From the structure of our neural network model (point 5 above), we can generate potential land cover maps activating or disactivating any of the four sources of variability. This enables to map each type of variability independently or together and to quantify their impact on the final estimations of the total land covered by bare ground, trees, and short vegetation.

Variability maps were produced by calculating the standard deviation of the prediction of each land cover at the pixel level for each source of variability independently (Fig S8). They were quantified in terms of area by assessing the total area of land covered by bare ground, trees, and short vegetation for each iteration.

A map propagating the variability associated to the choice of the climate source data, the spatial structure, and the model uncertainty was also generated in Fig S9.

9. Confidence interval of the median potential global fractional vegetation cover map.

The confidence interval for the prediction of each potential land cover type was calculated from the standard deviation of each land cover type resulting from the propagation of uncertainty of the model, from the influence of the spatial structure, and from the choice of the climate reference dataset. In total, we generated 600 maps per land cover type, with ten replicates for the model, ten folds for the spatial structure, and six climate reference datasets. One standard deviation map was produced for each land cover type (Fig S10). We then summed all the pixels values multiplied by their area to estimate the area concerned by the uncertainty. Here, we estimated that the area of land concerned by the uncertainty in bare ground cover equals 750 Mha, 895 Mha for the tree cover, and 1052 Mha for the short vegetation cover (Data File S1). The confidence interval (CI) was then calculated with the following equation:

$$\mathrm{CI} = z * \frac{\sigma_i}{\sqrt{\mathrm{n}}}$$

Considering a confidence interval of 95%, z equals 1.96; σ corresponds to the area concerned by the uncertainty of the land cover type i, and n (the number of land cover maps) equals 600. The confidence interval is therefore 60 Mha for the prediction of the potential bare ground cover, 72 Mha for the prediction of the potential tree cover, and 84 Mha for the prediction of the potential short vegetation cover.

10. The global potential of alternative ecosystems

We estimated the potential of alternative land cover by evaluating the standard deviation per pixel for each land cover type when changing the fire and herbivory scenario (Fig. 2). This map was generated using the full database, i.e., without considering the various sources of uncertainty considered in the present study. Here, we produced one map per climate reference dataset and per potential combination of fire regime and herbivory, i.e. considering the fire and herbivory values for the percentiles 5th, 25th, 50th, 75th and 95th per terrestrial ecoregion (Fig. S11).

Declarations

Acknowledgements. The authors would like to thank the following institutions for financial support: J.F.B. is supported by the Francqui foundation (Belgium) with a start-up grant, P.D., H.d.L, A.V.D are supported

by the FNRS (Belgium); F.B. is supported by the European Union's Horizon 2020 Research and Innovation Program under Marie Sklodowska-Curie Grant 845265; F.T.M. is supported by Universidad de Alicante (UADIF22-74 and VIGROB22-350) and Ministerio de Ciencia e Innovación of Spain (PID2020-116578RB-I00); J.C.S. is supported by Danish National Research Foundation (grant DNRF173), Independent Research Fund Denmark | Natural Sciences (grant 0135-00225B), Y.U. is supported by ARES.

Author contributions. J.F.B conceptualized the study. J.F.B and N.L performed the analysis. J.F.B led the writing of the manuscript with the contribution of C.G., F.B., F.M., J.C.S., J.B., E.A., S.B., T.B, S.B., T.d.H., H.d.L., P.D., M.D., A.H.v.D., P.L., S.L., G.M., C.M., D.M., M.P., A.P., F.Q., O.R., F.R., R.S., B.S., H.S., Y.T., Y.U., A.V.L.

Competing interests. The authors declare no competing interests.

Material and Correspondence. Correspondence and material requests should be addressed to jfbastin@uliege.be. Data and codes are available at Github: https://github.com/Nicolas-Latte/Alt_Pot_EcoSys

References and Notes

1. Steffen, W. *et al.* Planetary boundaries: Guiding human development on a changing planet. *Science (80-.).* **347**, (2015).
2. IPCC. *Climate Change 2022: Mitigation of Climate Change. Contribution of Working Group III to the Sixth Assessment Report of the Intergovernmental Panel on Climate Change*. (2022) doi:10.1017/9781009157926.
3. Cross, A. T., Nevill, P. G., Dixon, K. W. & Aronson, J. Time for a paradigm shift toward a restorative culture. *Restor. Ecol.* **27**, 924–928 (2019).
4. Bastin, J.-F. *et al.* The global tree restoration potential. *Science* **365**, 76–79 (2019).
5. Lewis, S. L., Wheeler, C. E., Mitchard, E. T. A. & Koch, A. Restoring natural forests is the best way to remove atmospheric carbon. *Nature* **568**, 25–28 (2019).
6. Moore, J. W. & Schindler, D. E. Getting ahead of climate change for ecological adaptation and resilience. *Science (80-.).* **376**, 1421–1426 (2022).
7. Veldman, J. W. *et al.* Tyranny of trees in grassy biomes. *Science (80-.).* **347**, 484–485 (2015).
8. Bastin, J.-F. *et al.* Response to Comments on "The global tree restoration potential". *Science* **366**, (2019).
9. Friedlingstein, P., Allen, M., Canadell, J. G., Peters, G. P. & I., S. S. Comment on "The global tree restoration potential" by Bastin, et al. *Science (80-.).* (2019).
10. Hoek van Dijke, A. J. *et al.* Shifts in regional water availability due to global tree restoration. *Nat. Geosci. 2022 155* **15**, 363–368 (2022).
11. Veldman, J. W. *et al.* Comment on 'The global tree restoration potential'. *Science (80-.).* (2019).

12. Pedersen, P. B. M., Ejrnæs, R., Sandel, B. & Svenning, J. C. Trophic Rewilding Advancement in Anthropogenically Impacted Landscapes (TRAAIL): A framework to link conventional conservation management and rewilding. *Ambio* **49**, 231–244 (2020).
13. Perring, M. P. *et al.* Advances in restoration ecology: Rising to the challenges of the coming decades. *Ecosphere* **6**, 131 (2015).
14. Stein, A., Gerstner, K. & Kreft, H. Environmental heterogeneity as a universal driver of species richness across taxa, biomes and spatial scales. *Ecol. Lett.* **17**, 866–880 (2014).
15. Garcia, C. A. *et al.* The Global Forest Transition as a Human Affair. *One Earth* **2**, 417–428 (2020).
16. Guirado, E. *et al.* Climate legacies drive the distribution and future restoration potential of dryland forests. *Nat. plants* **8**, 879–886 (2022).
17. Bastin, J.-F. *et al.* Understanding climate change from a global analysis of city analogues. *PLoS One* **14**, e0217592 (2019).
18. Garcia, A. *et al.* To Bend the Curve of Terrestrial Biodiversity, Place Agency Centre Stage. 29 (2020) doi:10.20944/preprints202010.0609.v1.
19. Suding, K. N., Gross, K. L. & Houseman, G. R. Alternative states and positive feedbacks in restoration ecology. *Trends Ecol. Evol.* **19**, 46–53 (2004).
20. Hobbs, R. J. *et al.* Managing the whole landscape: historical, hybrid, and novel ecosystems. *Front. Ecol. Environ.* **12**, 557–564 (2014).
21. Fløjgaard, C., Pedersen, P. B. M., Sandom, C. J., Svenning, J. C. & Ejrnæs, R. Exploring a natural baseline for large-herbivore biomass in ecological restoration. *J. Appl. Ecol.* **59**, 18–24 (2022).
22. Li, W. *et al.* Human fingerprint on structural density of forests globally. *Nat. Sustain. 2023 64* **6**, 368–379 (2023).
23. Jones, K. R. *et al.* One-third of global protected land is under intense human pressure. *Science* **360**, 788–791 (2018).
24. Pearce, E. A. *et al.* Substantial light woodland and open vegetation characterized the temperate forest biome before Homo sapiens. *Sci. Adv.* **9**, eadi9135 (2023).
25. Vancutsem, C. *et al.* Long-term (1990–2019) monitoring of forest cover changes in the humid tropics. *Sci. Adv.* **7**, (2021).
26. Berzaghi, F., Zhu, D., Alroy, J. & Ciais, P. Global distribution of mammal herbivore biomass reveals megafauna extinction patterns. *bioRxiv* 2021.10.19.464976 (2021) doi:10.1101/2021.10.19.464976.
27. Wang, L. *et al.* Tree cover and its heterogeneity in natural ecosystems is linked to large herbivore biomass globally. *One Earth* (2023) doi:10.1016/J.ONEEAR.2023.10.007.
28. Tölgyesi, C., Buisson, E., Helm, A., Temperton, V. M. & Török, P. Urgent need for updating the slogan of global climate actions from “tree planting” to “restore native vegetation”. *Restor. Ecol.* **30**, e13594 (2022).
29. Stein, A., Gerstner, K. & Kreft, H. Environmental heterogeneity as a universal driver of species richness across taxa, biomes and spatial scales. *Ecol. Lett.* **17**, 866–880 (2014).

30. Daskalova, G. N. & Kamp, J. Abandoning land transforms biodiversity. *Science (80-.).* **380**, 581–583 (2023).
31. Zimov, S. A., Schuur, E. A. G. & Chapin, F. S. Permafrost and the Global Carbon Budget. *Science (80-.).* **312**, 1612–1613 (2006).
32. Gordon, C. E. *et al.* Elephant rewilding affects landscape openness and fauna habitat across a 92-year period. *Ecol. Appl.* **33**, e2810 (2023).
33. Mirzabaev, A., Sacande, M., Motlagh, F., Shyrokaya, A. & Martucci, A. Economic efficiency and targeting of the African Great Green Wall. *Nat. Sustain. 2021 51* **5**, 17–25 (2021).
34. Purves, D. & Pacala, S. Predictive models of forest dynamics. *Science (80-.).* **320**, 1452–1453 (2008).
35. Davoli, M. *et al.* Megafauna diversity and functional declines in Europe from the Last Interglacial to the present. *Glob. Ecol. Biogeogr.* **00**, 1–14 (2023).
36. Bastin, J.-F. *et al.* The extent of forest in dryland biomes. *Science* **356**, 635–638 (2017).
37. Bey, A. *et al.* Collect earth: Land use and land cover assessment through augmented visual interpretation. *Remote Sens.* **8**, 1–24 (2016).
38. Marius-Constantin, P., Balas, V. E., Perescu-Popescu, L. & Mastorakis, N. Multilayer perceptron and neural networks. *WSEAS Trans. Circuits Syst.* **8**, 579–588 (2009).
39. UNESCO. The World Database on Protected Areas. https://www.protectedplanet.net/c/world-database-on-protected-areas (2011).
40. Jones, K. R. *et al.* One-third of global protected land is under intense human pressure. *Science* **360**, 788–791 (2018).
41. Fick, S. E. & Hijmans, R. J. WorldClim 2: new 1-km spatial resolution climate surfaces for global land areas. *Int. J. Climatol.* **37**, 4302–4315 (2017).
42. Copernicus Climate Change Service (C3S). ERA5: Fifth generation of ECMWF atmospheric reanalyses of the global climate. Copernicus Climate Change Service Climate Data Store (CDS). https://cds.climate.copernicus.eu/cdsapp#!/home (2017).
43. Harris, I., Osborn, T. J., Jones, P. & Lister, D. Version 4 of the CRU TS monthly high-resolution gridded multivariate climate dataset. *Sci. Data 2020 71* **7**, 1–18 (2020).
44. Karger, D. N. *et al.* CHELSA-W5E5: Daily 1gkm meteorological forcing data for climate impact studies. *Earth Syst. Sci. Data* **15**, 2445–2464 (2023).
45. Wan, Z., S. Hook, G. H. MODIS/Aqua Land Surface Temperature/Emissivity 8-Day L3 Global 1km SIN Grid V061. *NASA EOSDIS Land Processes Distributed Active Archive Center* https://doi.org/10.5067/MODIS/MYD11A2.061 (2021).
46. Chavent, M., Kuentz-Simonet, V., Liquet, B. & Saracco, J. ClustOfVar: An R Package for the Clustering of Variables. *J. Stat. Softw.* **50**, 1–16 (2012).
47. Hengl, T. *et al.* SoilGrids250m: Global gridded soil information based on machine learning. *PLoS One* **12**, e0169748 (2017).

48. Danielson, J. J. & Gesch, D. B. *Global multi-resolution terrain elevation data 2010 (GMTED2010). Open-File Report* https://pubs.er.usgs.gov/publication/ofr20111073 (2011) doi:10.3133/OFR20111073.
49. Giglio, L., C. Justice, L. Boschetti, D. R. MODIS/Terra+Aqua Burned Area Monthly L3 Global 500m SIN Grid V061. *NASA EOSDIS Land Processes Distributed Active Archive Center* https://doi.org/10.5067/MODIS/MCD64A1.061. (2021).
50. Valavi, R., Elith, J., Lahoz-Monfort, J. J. & Guillera-Arroita, G. blockCV: An r package for generating spatially or environmentally separated folds for k-fold cross-validation of species distribution models. *Methods Ecol. Evol.* **10**, 225–232 (2019).
51. Thrasher, B., Maurer, E. P., McKellar, C. & Duffy, P. B. Technical Note: Bias correcting climate model simulated daily temperature extremes with quantile mapping. *Hydrol. Earth Syst. Sci.* **16**, 3309–3314 (2012).
52. Olson, D. M. *et al.* Terrestrial Ecoregions of the World: A New Map of Life on EarthA new global map of terrestrial ecoregions provides an innovative tool for conserving biodiversity. *Bioscience* **51**, 933–938 (2001).
53. *Materials and methods are available as supplementary materials.*

Supplementary Data File

Supplementary Data File S1 is not available with this version.

Figures

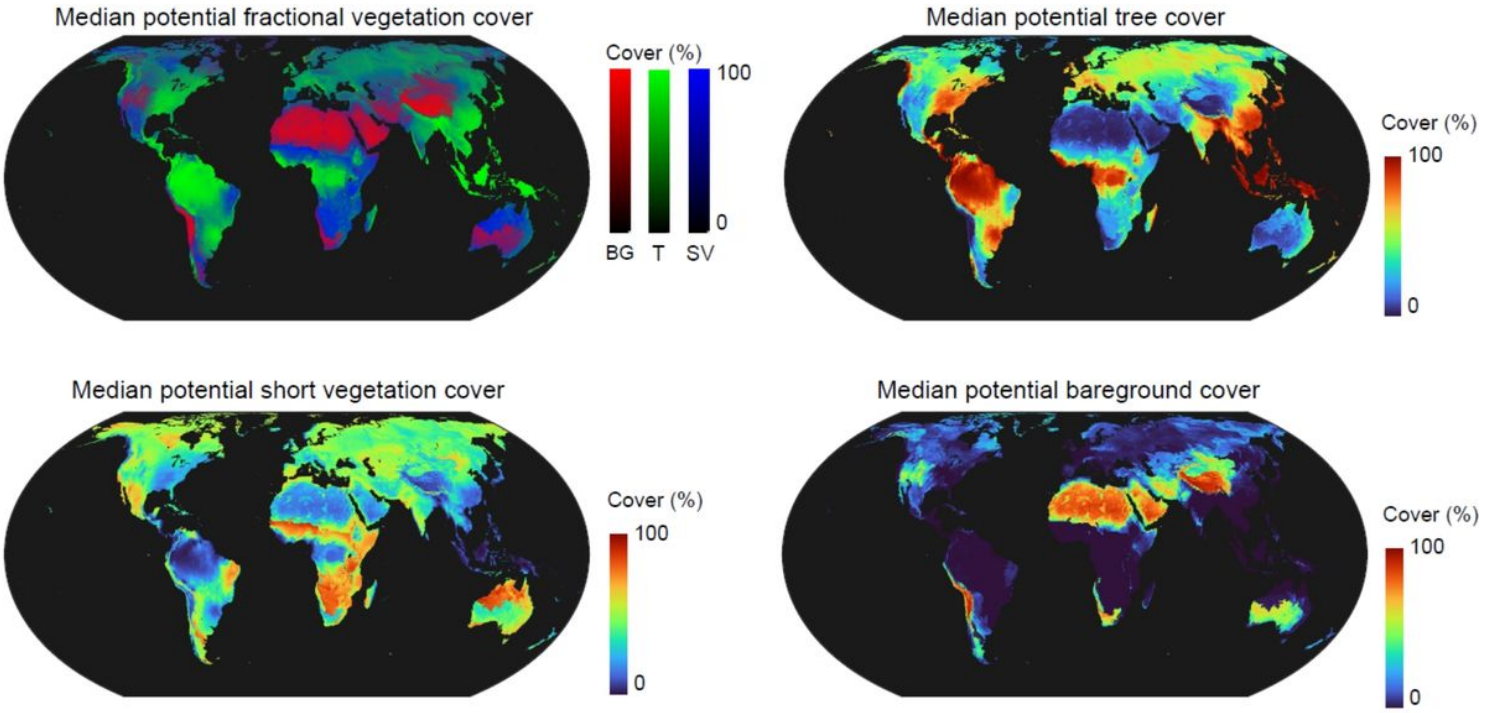

Figure 1

The global potential fractional vegetation cover. The map displays the median potential fractional vegetation cover per pixel, based on the observed fire regime and herbivory per ecoregion within protected areas of IUCN class I, II, and III. The sum of potential tree (T), short vegetation (SV), and bareground (BG) cover (top left) equals 100% for each pixel. The remaining subfigures display each potential land cover separately for enhanced clarity.

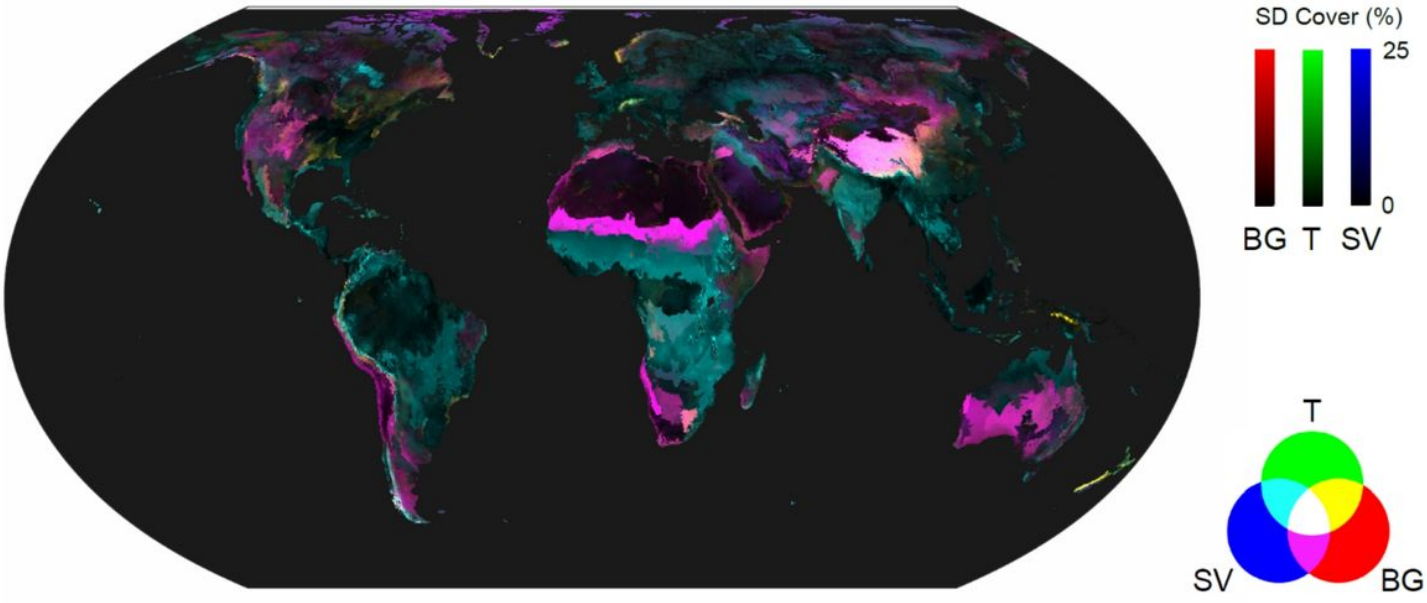

Figure 2

Global map of potential alternative ecosystems. This map depicts the potential for alternative ecosystems on a global scale, based on the changes in fire regime (prescribed or excluded) and herbivore intensity scenarios [53]. Each pixel of the map represents the standard deviation (SD) of the predictions for bare ground (BG), tree (T) and short vegetation (SV) cover. The resulting additive color rendering corresponds to pixels where alternatives are found between two dominant land cover types (cyan for trees and short vegetation, magenta for short vegetation and bareground, and in yellow for trees and bareground). A Venn diagram summarizes this color legend.

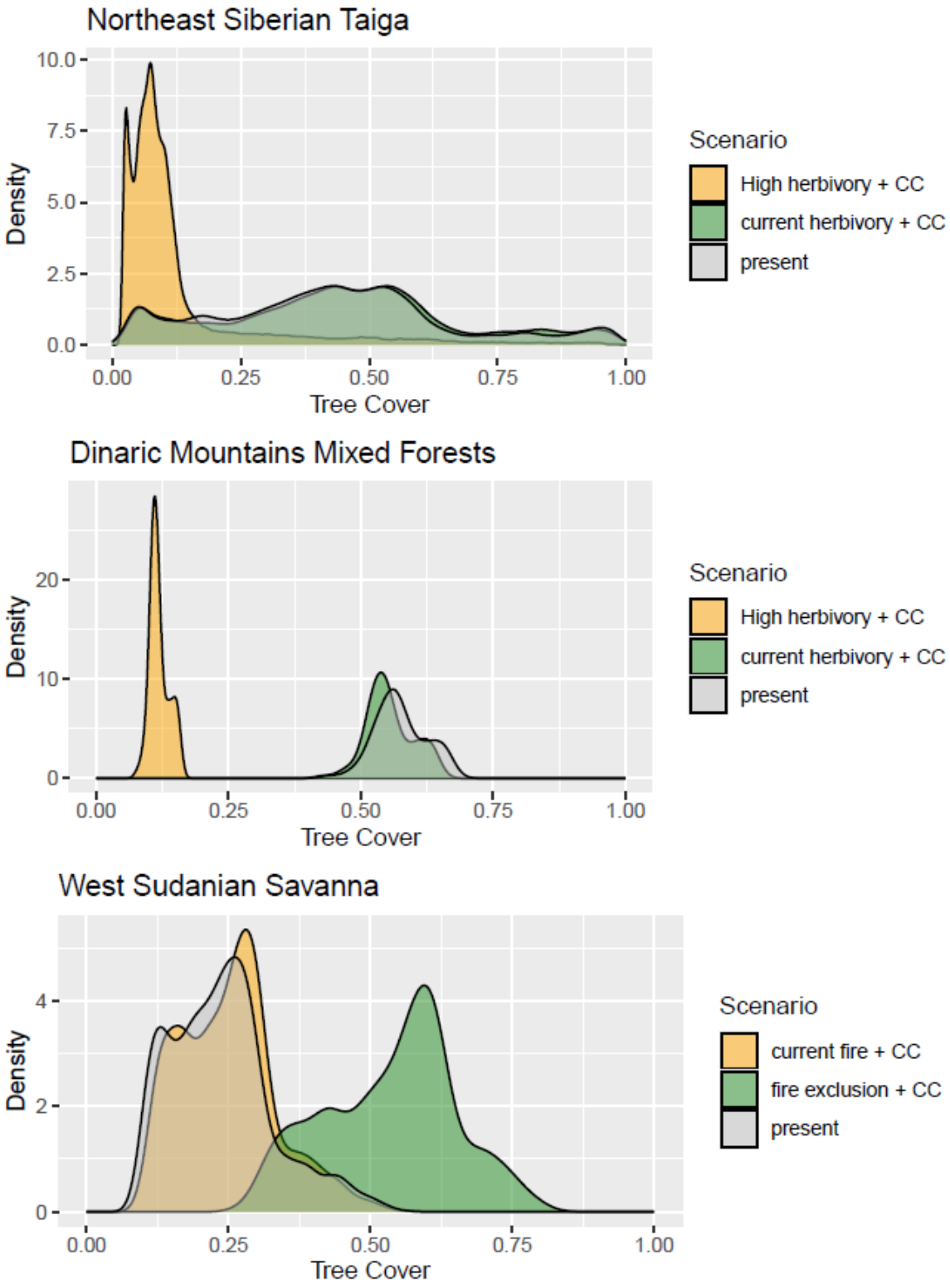

Figure 3

Examples of potential alternative tree cover distributions resulting from different management scenarios and climate change at the ecoregion level. The effect of three scenarios (fire, herbivory, and climate change SSP5 [CC]) is illustrated on the potential tree cover of three ecoregions, i.e. the Northeast Siberian Taiga, the Dinaric Mountains Mixed Forests and the West Sudanian Savanna. Each panel compares different scenarios including (i) the current potential without changing the fire regime, herbivory, or

climate change, (ii) the current herbivory biomass and the expected climate change by 2050 (current herbivory + CC), (iii) 30 tons of herbivory biomass per km^2 and the expected climate change by 2050 (high herbivory + CC), (iv) the current fire regime and the expected climate change by 2050 (current fire + CC), and (v) a prescribed fire of 0.5 yr^{-1} and the expected climate change by 2050 (fire exclusion + CC).

Supplementary Files

This is a list of supplementary files associated with this preprint. Click to download.

- SupplementaryTableandFigures.docx